Electronic Supplementary Material (ESI) for Nanoscale.

Supporting Information

Engineering Graphene with Red Phosphorus Quantum Dots for Superior Hybrid Anodes of Sodium-ion Batteries

Guang Zeng,[a,b] Xiang Hu,[a,b] Baolong Zhou,[a,b] Junxiang Chen,[a,b] Changsheng Cao,[a,b] and Zhenhai Wen*,[a,b]

[a] Key Laboratory of Design and Assembly of Functional Nanostructures, Fujian Institute of Research on the Structure of Matter, Chinese Academy of Sciences, Fuzhou 350002, P. R. China

[b] Fujian Provincial Key Laboratory of Nanomaterials, Fujian Institute of Research on the Structure of Matter, Chinese Academy of Sciences, Fuzhou 350002, P. R. China

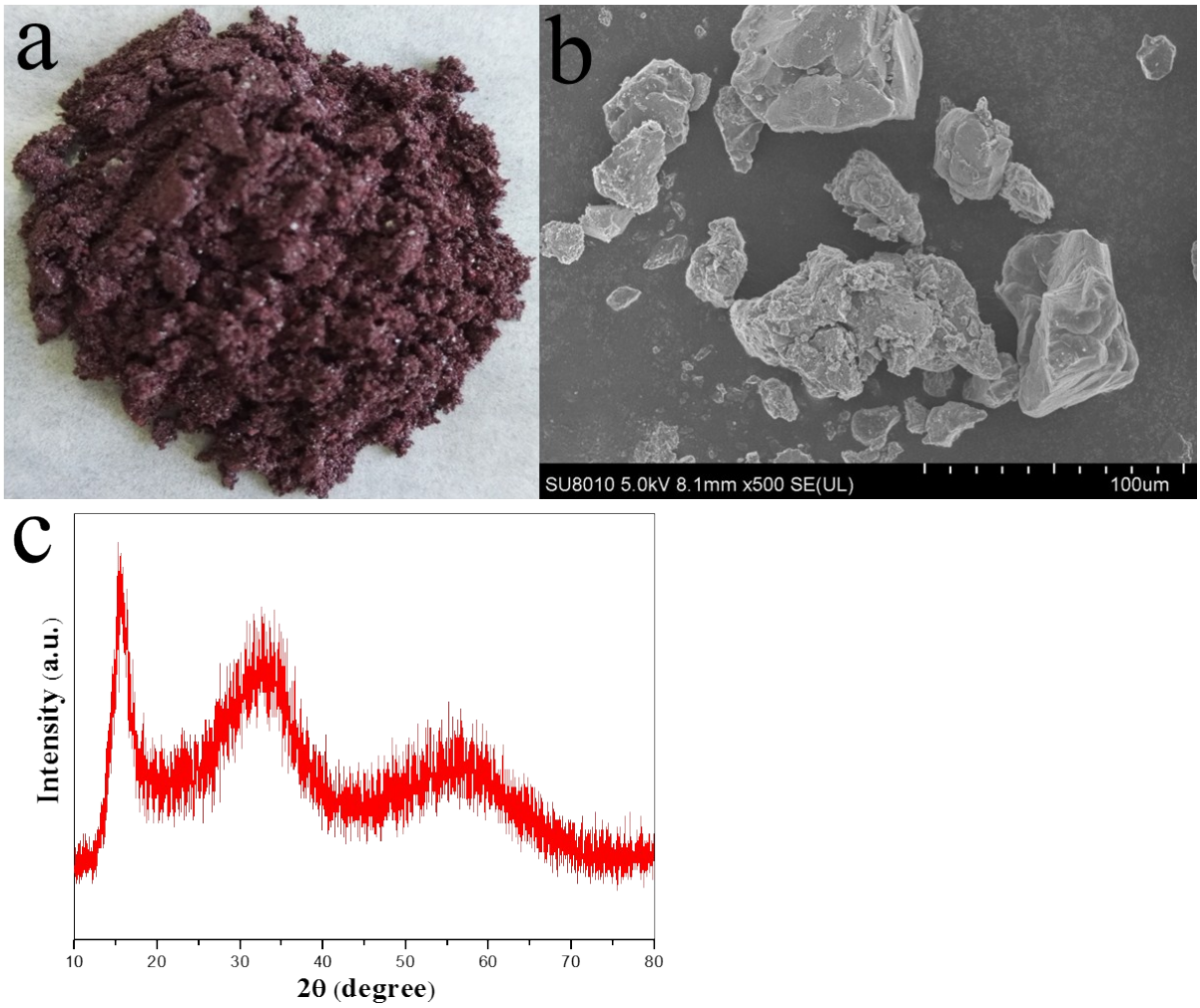

Figure S1. (a) Photo image, (b) SEM image and (c) XRD pattern of the commercial red phosphorus.

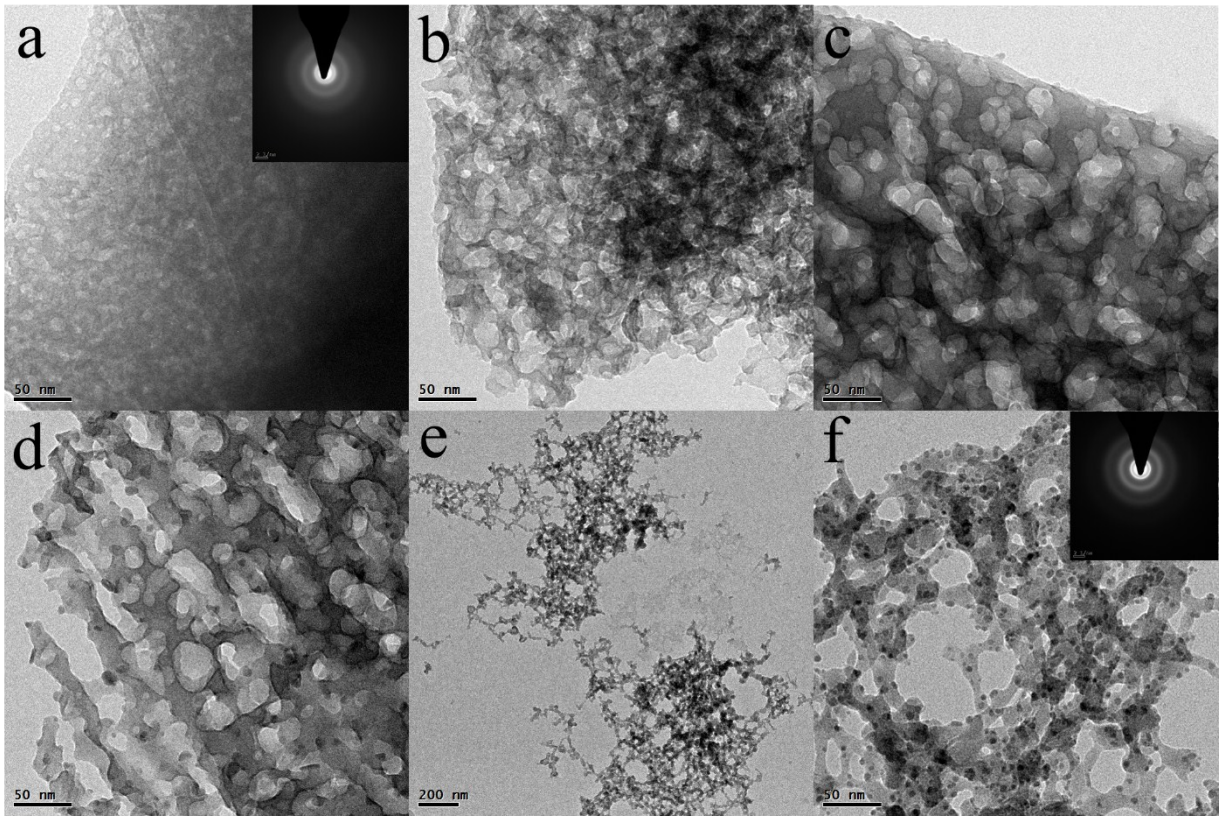

Figure S2. TEM images of red phosphorus after hydrothermal treatment at 200 °C for different time. (a) 2 h, (b) 6 h, (c) 12 h, (d) 18 h, and (e, f) 24 h. The insets are the SEAD patterns related to the red phosphorus after hydrothermal treatment at 200 °C for 2 h and 24 h, respectively.

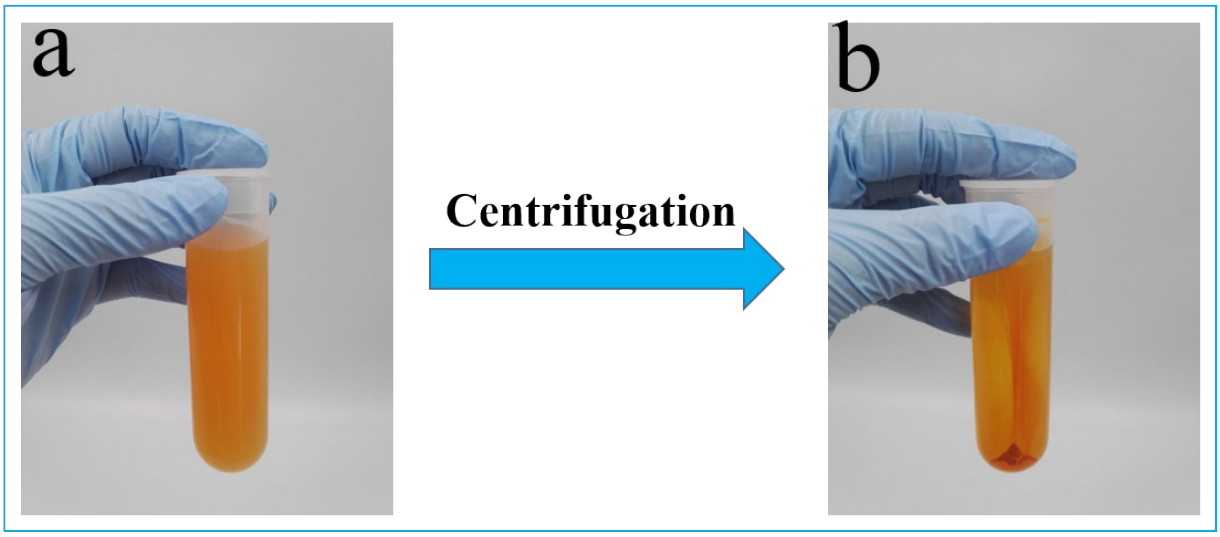

Figure S3. Optical images showing the separation process of RPQDs from RPNWs. (a) Digital camera image of ultracentrifuge tubes containing RPQDs and RPNWs solution; (b) Digital camera image of ultracentrifuge tubes containing RPQDs solution and RPNWs sedimentation after centrifugation at 8000 rpm for 30 min. After centrifugation, the 2/3 supernatant containing RPQDs was decanted.

Table S1. Zeta potential of GO and RPQDs after PAH modification.

Materials	GO	RPQDs
Zeta potential (mV)	-33.51	32.56

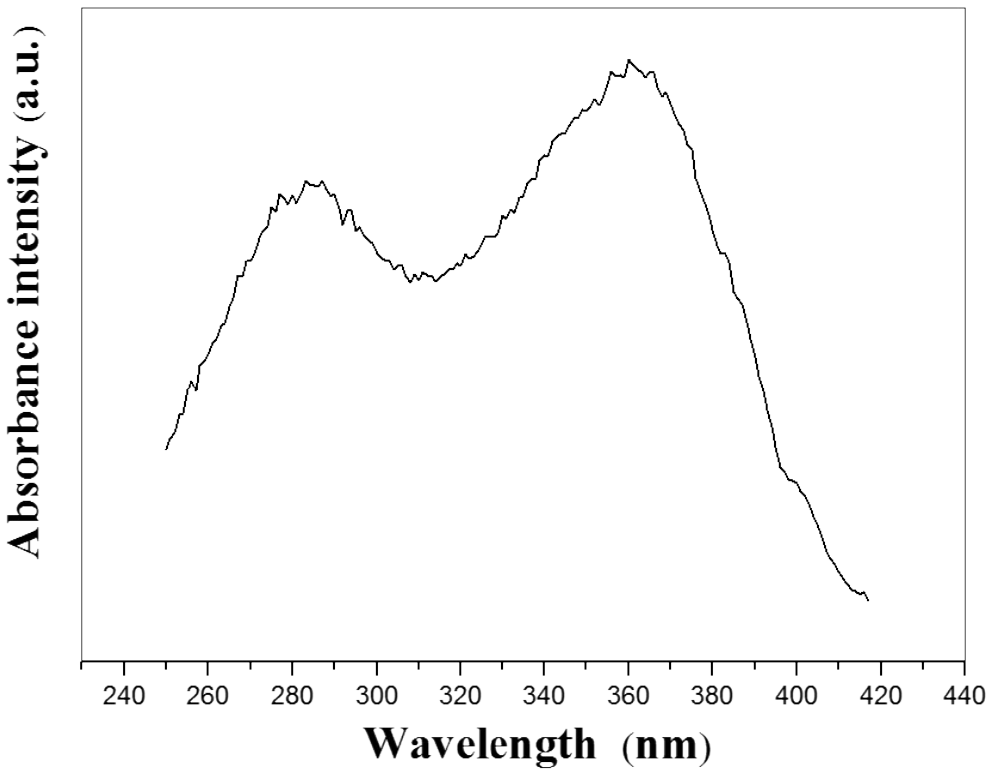

Figure S4. UV/Vis adsorption spectrum of RPQDs in water.

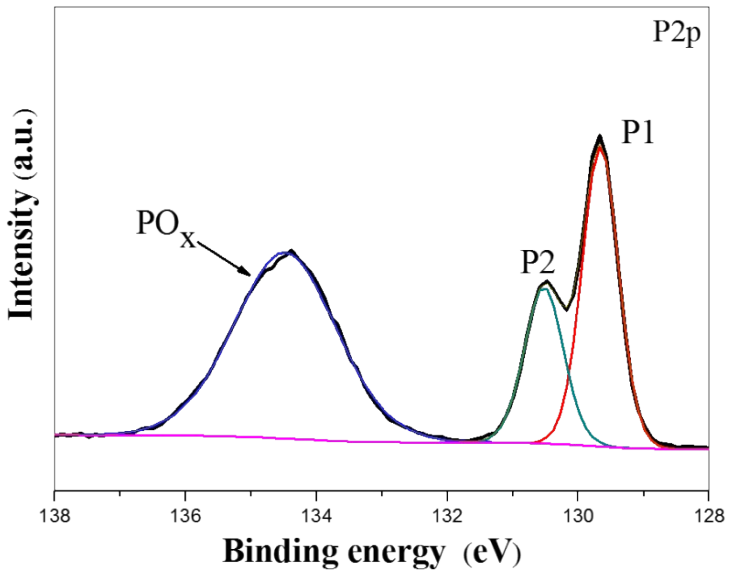

Figure S5. P2p XPS spectrum of commercial red phosphorus.

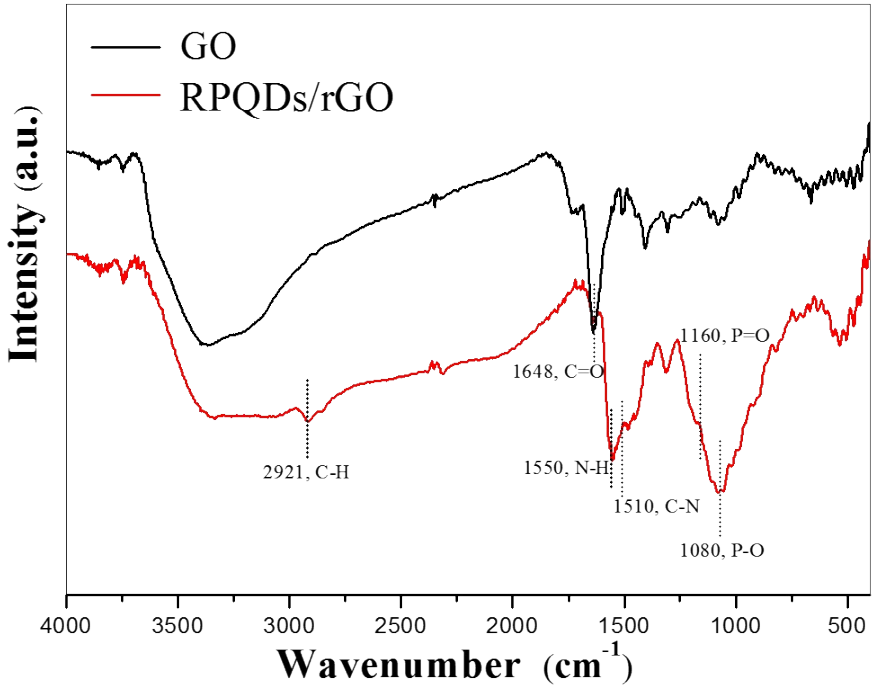

Figure S6. FT-IR spectra of GO and RPQDs/rGO hybrid.

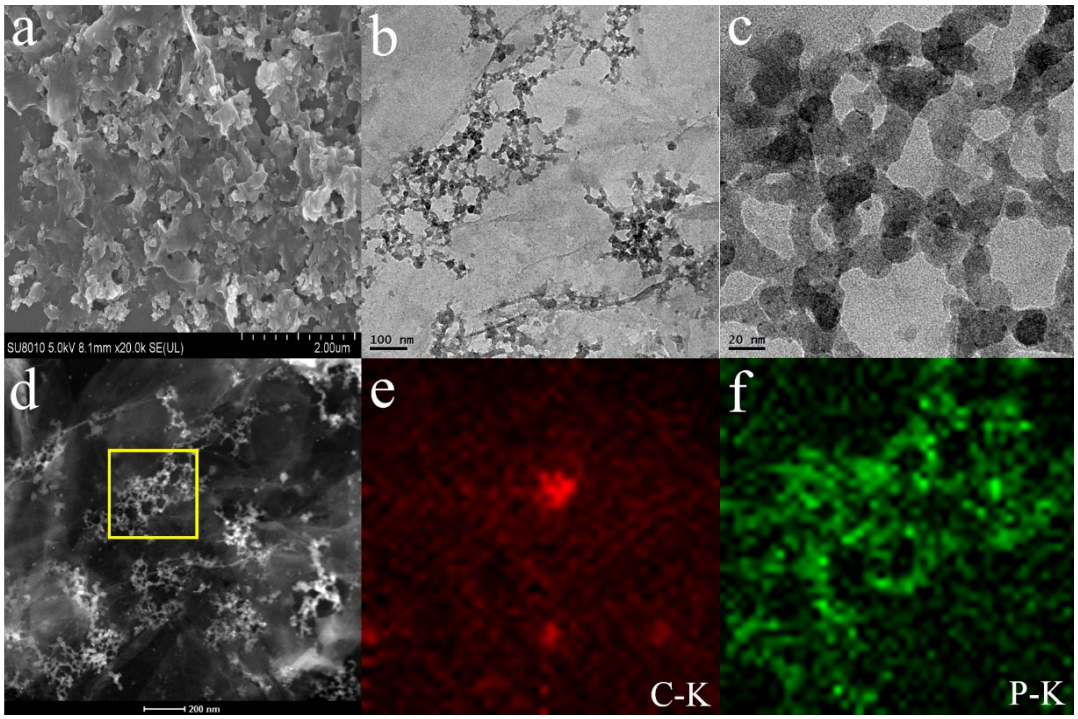

Figure S7. (a) SEM images of RPNWs/rGO hybrid; (b), (c) TEM images of RPNWs/rGO hybrid; (d) High angle annular dark-field STEM (HAADF-STEM) image and corresponding carbon (e) and phosphorus (f) elemental mappings of RPNWs/rGO hybrid.

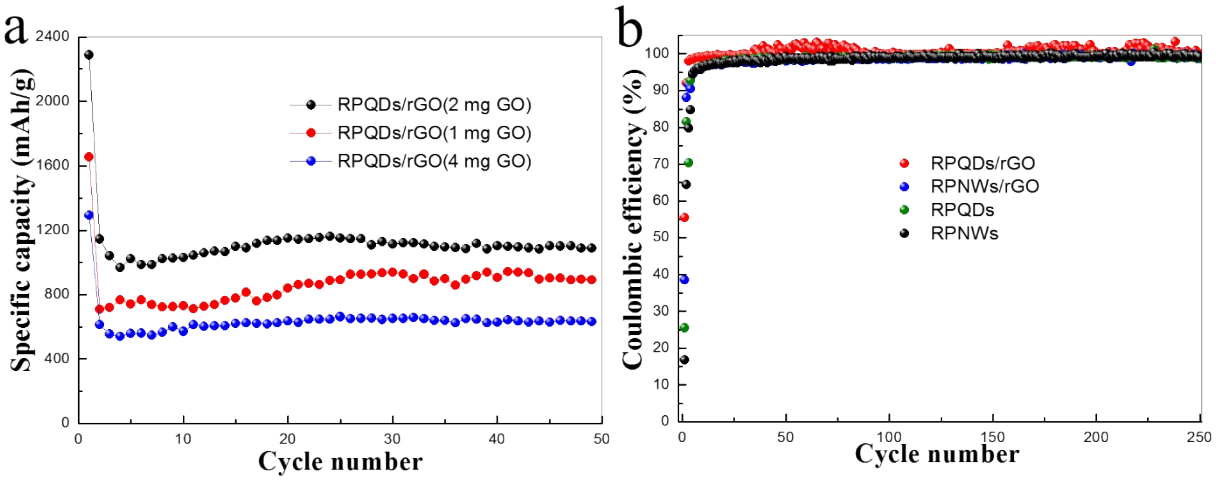

Figure S8. (a) Cycling performances of RPQDs/rGO electrodes with different GO addition during preparation process at a current density of 200 mA g^{-1} cycled between 0.005 and 2.0 V vs. Na^+/Na; (b) Coulombic efficiency of RPQDs/rGO hybrid, RPNWs/rGO hybrid, RPQDs and RPNWs electrodes at a current density of 200 mA g^{-1}.

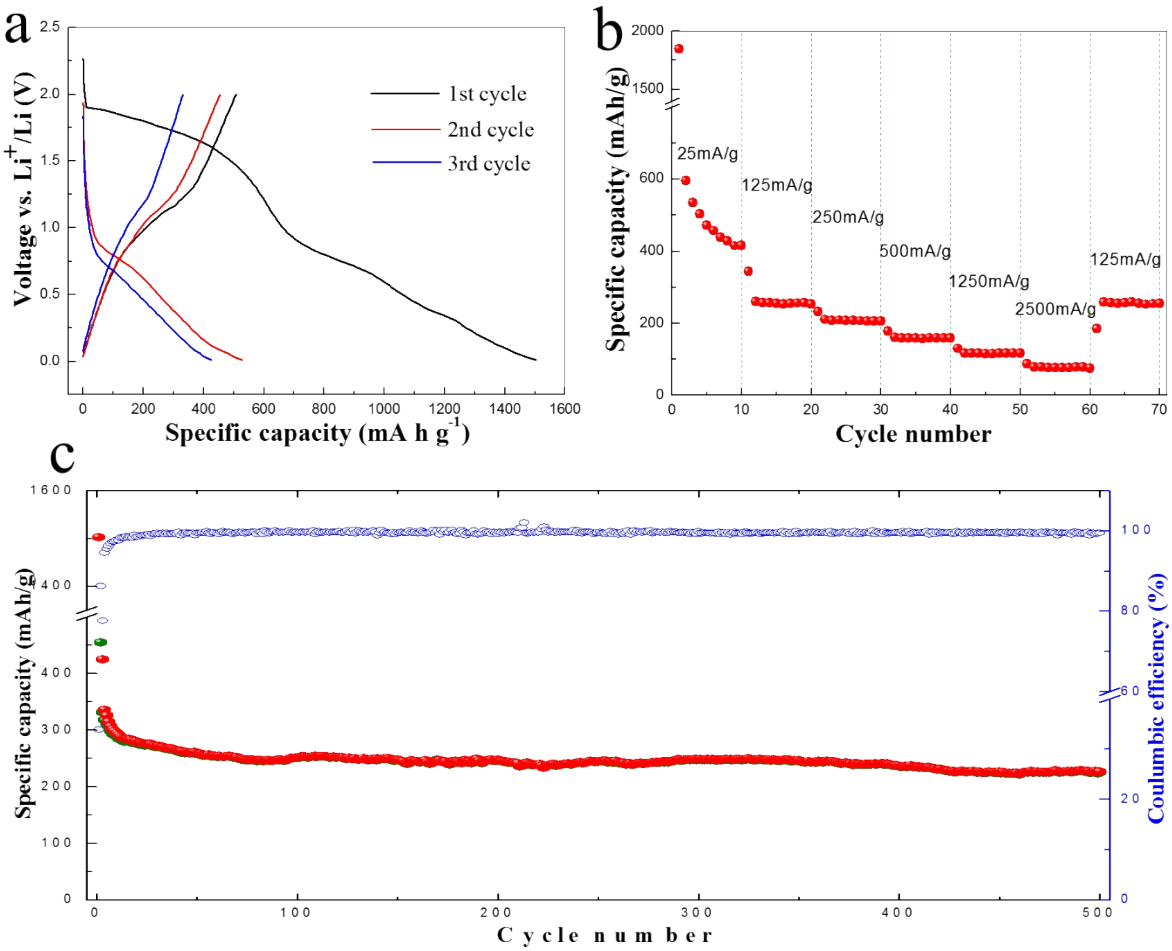

Figure S9. (a) Discharge-charge profiles of RPQDs at a current density of 125 mA g^{-1} for LIBs cycled between 0.005 and 2.0 V vs Li^+/Li; (b) Rate performance of RPQDs electrode for LIBs; (c) Cycling performances of RPQDs with a current density of 125 mA g^{-1} for LIBs cycled between 0.005 and 2.0 V vs Li